

ELECTRO-MECHANICAL RESPONSE OF STRETCHABLE PDMS COMPOSITES WITH A HYBRID FILLER SYSTEM

Haeji Kim¹, Nadeem Qaiser², Byungil Hwang¹

¹School of Integrative Engineering, Chung-Ang University, Republic of Korea

²Material Science and Engineering, Physical Science and Engineering Division, King Abdullah University of Science and Technology (KAUST), Saudi Arabia

Abstract. *With the technological development of wearable devices, there are increasing demands for stretchable conductor that have stable electro-mechanical performance. In this study, a stretchable PDMS composite electrodes using ternary systems of fillers consisting of poly(3,4-ethylenedioxythiophene):poly(styrenesulfonate) (PEDOT:PSS) / carbon nanotube (CNT) / silver nanowire (AgNW) is explored in a perspective of electro-mechanical response. PDMS matrix is mixed with binary fillers of CNT and PEDOT:PSS, which is followed by AgNW peeling-off process. The PDMS composite is mechanically reliable especially under tensile deformation, which showed a high rupture strain of ~102% and tensile strength of ~2.7 MPa. In addition, the PDMS composites shows the stable electro-mechanical response, where high electrical conductivity is sustained even under stretchable conditions, showing an electrical resistance value of ~11.7 Ω /cm under 40% of strain. As a demonstration, a supercapacitor using the PDMS composites is demonstrated that shows reliable electrochemical performance.*

Key words: *Electro-mechanical response, Composite, Tensile deformation, Strength, Conductivity*

1. INTRODUCTION

Stretchable electronics have attracted much attention for futuristic devices such as wearable health care sensors [1-3], energy harvesting or storage systems [4-7], and data processing devices [8, 9]. A key component of developing a stretchable electronic device is a stretchable conductor that is mechanically reliable under repeated tensile or compressive deformation [10]. There are two main trends to fabricate stretchable conductors: 1) utilizing all stretchable materials [11, 12] and 2) bridging rigid components

Received: December 05, 2022 / Accepted: January 15, 2023

Corresponding author: Byungil Hwang

School of Integrative Engineering, Chung-Ang University, 84 Heukseok-Ro, Dongjak-Gu, Seoul 06974, Republic of Korea

E-mail: bihwang@cau.ac.kr

with stretchable interconnects [13-16]. The thin metal film electrodes patterned to have serpentine structure is the representative example for the latter case of the stretchable interconnects [17]. The serpentine-structured metal electrodes interconnect the Si-based electronic components having excellent device performances while releasing the imposed mechanical strain by accommodating their geometry under deformation, thereby realizing stretchable and ultra-high-performance electronic devices [18]. Despite the advantages of the method utilizing patterned metal interconnects, the use of such methods for electronic devices is limited due to the complex fabrication process using a multistep lithography process [19]. On the other hand, the fabrication of composite films by mixing functional fillers with the stretchable matrix is the most widely used strategy to fabricate the stretchable conductor in the former case [12, 20-23]. The composite films with different properties can be fabricated by introducing different types of functional fillers, which allowed the fabrication of various electronic devices [20, 24, 25]. For example, Lee et al. fabricated a stretchable conductor by integrating silver nanowires (AgNWs) and graphene with polydimethylsiloxane (PDMS), which showed a rupture strain of 100% [26]. In the work by Shi et al, graphene hybridized CNT film with PDMS matrix for wearable sensors that resists under cyclic mechanical strain was developed [27]. Gallium-based liquid metal alloy (EGaIn) is used as a conductive filler as well. Gallium and Indium are mixed in a ratio of 3:1 desirably and directly mixed with liquid metal-filled magnetorheological elastomer (LMMRE), showing high electrical conductivity and mechanical deformability [28]. However, more research related to electro-mechanical response is needed for use in stretchable electronic systems for wearable devices.

In our previous study, the hybrid system of poly(3,4-ethylenedioxythiophene):poly(styrenesulfonate) (PEDOT:PSS), carbon nanotubes (CNTs), and AgNWs was proposed as the supercapacitor materials, which acted as pseudocapacitor, electrical double layer (EDL), and current collector materials, respectively [29]. In this system, the advantages of a pseudocapacitor with high energy density and EDL with high power density were combined, thereby exhibiting excellent supercapacitor performances [30]. In addition, the high electrical conductivity of the AgNW network-based current collector optimized the supercapacitor performances [31]. However, the layers of PEDOT:PSS, CNTs, and AgNWs were deposited on silk fiber as a form of the thin film; thus, the use of the supercapacitor for stretchable devices was limited.

In this study, we demonstrated mechanically stable conductive PDMS composites using the hybrid system of PEDOT:PSS, CNTs, and AgNWs as functional fillers. As commented above, the hybrid system took benefits of each materials, where pseudocapacitor and EDL characteristics were come from PEDOT:PSS and CNT, respectively. A simple blending and peeling-off method were used to fabricate the composites where molten PDMS was mixed with PEDOT:PSS and CNTs and then was coated with AgNWs. To improve the conductivity of PEDOT:PSS, ethylene glycol (EG) was added to PEDOT:PSS solution as a doping agent. The water-soluble PEDOT:PSS was able to be mixed with the hydrophobic PDMS by reducing the hydrophobicity of PDMS aided by the surfactant, Triton X-100. Tensile tests were performed on the PDMS composites with different filler contents, enhancing the composition of the matrix and filler materials. The mechanical failure mechanism of the PDMS composites with the varying filler composites was also investigated by microstructural analysis using scanning electron microscopy (SEM). The electrochemical performance of the optimized PDMS composites with the hybrid fillers of

PEDOT:PSS, CNTs, and AgNWs was characterized and confirmed the potential of the demonstrated composites for a stretchable supercapacitor.

2. MATERIALS AND METHODS

2.1. Fabrication of CNT/PDMS/PEDOT:PSS Composites

CNT (Jeno Tube 6A, JEIO) was first dispersed in a deionized (DI) water with the surfactant, sodium dodecylbenzene sulfonate (50.0%, SDBS, Samcheon Chemical Co. Ltd, Korea). Then, a tip sonicator was used to disperse CNT more uniformly at 60% amplitude of 500 W and 20 kHz for 10 min with a 3 mm diameter tip. PEDOT:PSS, EG (Sigma Aldrich), and Triton X-100 (DAEJUNG, Korea) were blended together using a magnetic bar at 450 rpm for 1 h. After that, the mixed PEDOT:PSS, EG, and Triton X-100 added to the dispersed CNT was evaporated on a hot plate at 150 °C for 20 min. The solvent-removed mixture of functional fillers (CNT/PEDOT:PSS), and PDMS (Sylgard-184, Dow Corporation, Michigan, USA) was blended in a planetary vacuum mixer (ARV-310, THINKY Corporation, Tokyo, Japan) at 2000 rpm under 20 kPa for 5 min with a curing agent. AgNW solution (Flexiowire 2020, SG Flexio Co. Ltd, Korea) was coated on a polytetrafluoroethylene (PTFE) casting molds (8.0 (w) × 48.0 (l) × 0.3 mm (t) and 40.0 (w) × 30.0 (l) × 0.3 mm (t)) at 100 °C for 1 h in an oven. The previously mixed CNT/PEDOT:PSS/PDMS composite blend was then poured on the surface of AgNW-coated PTFE mold. Prior to the curing process, the CNT/PEDOT:PSS/PDMS composite blend was degassed in a vacuum at room temperature under a 15 kPa for 2 h and later cured in a vacuum oven at 100 °C for 6 h. The AgNW-coated CNT/PEDOT:PSS/PDMS composite was fabricated via the peeling-off method from the PTFE mold.

2.2. Characterization

Field-Emission Scanning Electron Microscopy (FE-SEM; SIGMA, Carl Zeiss AG, Oberkochen, Germany) was utilized to analyze the surface and cross-section morphologies of the fabricated composite. A rheometer (Compac-100II, Sun Scientific Co. Ltd., Tokyo, Japan) was used for tensile testing under a maximum load cell of 100 N with a table speed of 120 mm/min. A high-resolution drop shape analyzer (DSA 100, KRÜSS GmbH) was utilized to evaluate the contact angle of the fabricated sample to analyze its wettability. A battery cycler system (WBCS3000L, WonATech, Seoul, Korea) was used to measure the electrochemical property of the composite by cyclic voltammetry (CV).

3. RESULTS AND DISCUSSION

Fig. 1 illustrates the fabrication process of the AgNW-coated CNT/PEDOT:PSS/PDMS composites. First, CNTs were dispersed in DI water by using a tip sonicator (Fig. 1a). The CNTs having hydrophobic surface tend to be agglomerated in hydrophilic DI water. Therefore, an anionic surfactant, sodium dodecyl benzene sulfonate (SDBS) was added, where amphiphilic SDBS enhanced the dispersion of CNT in DI water (inset of Fig. 1a) [32]. Afterward, the remaining solvent was removed through the drying process. Next, PEDOT:PSS solution was mixed with Triton X-100 and EG through stirring (Fig. 1a). The

weight fraction of the PEDOT:PSS solution was varied from 0 to 20 wt%, in order to examine the effect of the concentration of PEDOT:PSS on the stretchability of the composites. 15 wt% of PEDOT:PSS solution was used for all the composites of this study because more than 15 wt% of PEDOT:PSS dramatically degraded the stretchability (Fig. 2). The high content of PEDOT:PSS caused the mechanical rupture at the much lower strain than those with low content of PEDOT:PSS as shown in Fig. 2. The early rupture resulted in the low strength value. EG was added to increase the size of the conductive grain, cause agglomeration, and increase the carrier mobility, enhancing the electrical conductivity of the PEDOT:PSS [11]. Moreover, it disconnects the insulating PSS part from PEDOT:PSS which results in a further increase of the conductivity [33]. Triton X-100 serves as a surfactant, which allows for hydrophilic PEDOT:PSS to be mixed with hydrophobic PDMS [34]. The mixture of PEDOT:PSS/EG/Triton X-100 and the treated CNTs were then mixed with the PDMS and curing agent by using a planetary vacuum mixer (Fig. 1b). AgNWs were coated on the fabricated polymer blend film via a peeling-off method to further decrease the resistance, leading the film to have higher electrical conductivity. Here, AgNW solution was first poured on the PTFE casting mold followed by drying in an oven (Fig. 1c). Lastly, the mixture of CNT/PEDOT:PSS/PDMS was poured on the AgNW-coated PTFE mold. AgNW was embedded to the molten mixture of CNT/PEDOT:PSS/PDMS, causing stronger adhesion between the two layers. In order to eliminate the air bubbles in the composites, degassing process was performed, which was then cured in a vacuum oven (Fig. 1d). By peeling off the cured composite from the PTFE mold, the stretchable AgNW/CNT/PEDOT:PSS/PDMS composite electrode was fabricated (Fig. 1e).

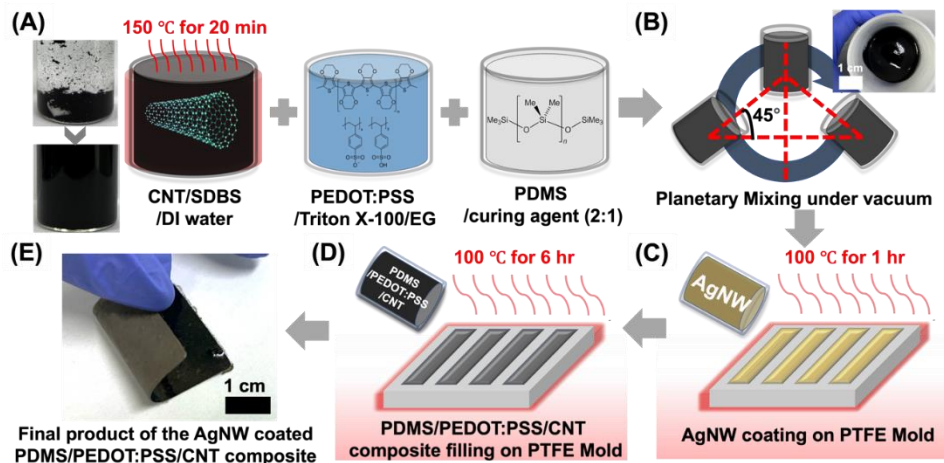


Fig. 1 Schematic illustration of the fabrication process of the AgNW coated CNT/PEDOT:PSS/PDMS composite.

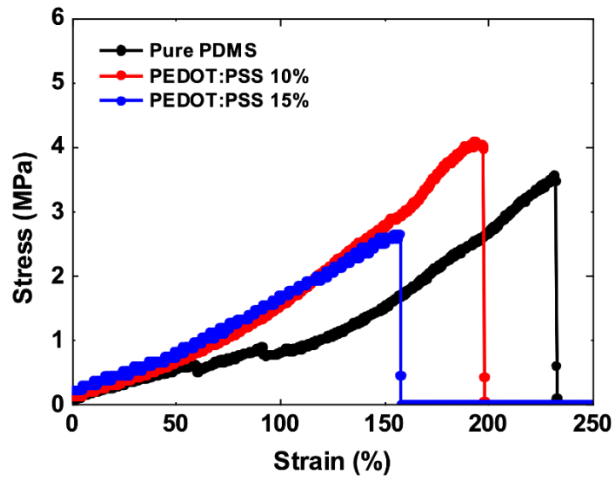


Fig. 2 Stress-strain curves of PDMS composites with the different PEDOT:PSS contents.

Fig. 3 shows the cross-sectional SEM images of the composites with different fillers. Pure PDMS (Fig. 3a) and PEDOT:PSS/PDMS (Fig. 3b) showed smooth surface indicating that the PEDOT:PSS was homogeneously dispersed in PDMS without severe agglomeration. In the CNT/PEDOT:PSS/PDMS composites (Fig. 3c), the CNTs were distributed through the bulk part of the composites and no severe agglomerated CNTs were observed. This confirmed that our dispersion method for CNTs and PDMS was effective to fabricate the uniform CNT/PEDOT:PSS/PDMS composites. In Fig. 3d, AgNWs were embedded on the surface of CNT/PEDOT:PSS/PDMS composites. During the curing step, AgNWs on the PTFE mold were partially immersed in the mixture of CNT/PEDOT:PSS/PDMS, which was then bound to the PDMS matrix forming the partially embedded AgNW networks.

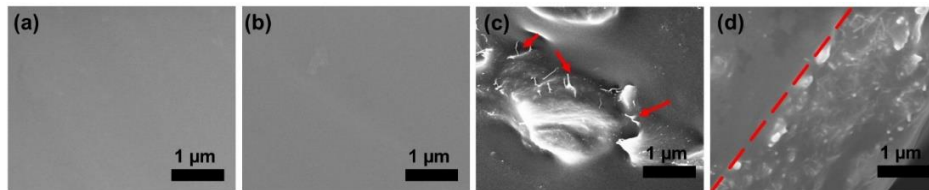


Fig. 3 Cross-sectional SEM images of (a) pure PDMS, (b) PEDOT:PSS/PDMS composite, (c) CNT/PEDOT:PSS/PDMS composite (the arrow indicates the presence of CNT), and (d) AgNW-coated CNT/PEDOT:PSS/PDMS composite (dash line indicates the boundary between AgNW and the CNT/PEDOT:PSS/PDMS mixture).

Fig. 4a shows the stress-strain curves of the various composites mixed with a different mixture of fillers, which were pure PDMS, PDMS/PEDOT:PSS, CNT/PDMS/PEDOT:PSS, and AgNW-coated CNT/PDMS/PEDOT:PSS, respectively. The failure stress and strain decreased as the fillers were added. Pure PDMS exhibited a strain and stress of ~235% and ~3.7 MPa, respectively, which were decreased to ~165% and ~2.8 MPa, respectively, with the addition of 15 wt% of PEDOT:PSS. The CNT/PDMS/PEDOT:PSS showed a further

decrease in strain and stress values showing ~102% and ~2.7 MPa, respectively. The coating of AgNW on the surface of PDMS/PEDOT:PSS/CNT composite showed similar stress and strain values compared to those of the PDMS/PEDOT:PSS/CNT composites. The addition of the brittle PEDOT:PSS resulted in the decreased volume fraction of the stretchable PDMS in the composites. Thus, the PEDOT:PSS/PDMS composites showed lower stretchability than those of pure PDMS. The addition of CNTs further decreased the volume fraction of PDMS, which resulted in the poorer stretchability of CNT/PEDOT:PSS/PDMS composites than those of PEDOT:PSS/PDMS composites. In addition, the applied stress can be localized at the interface between CNTs and PDMS, which further degrades the stretchability. However, the partial embedding of AgNWs only on the surface of the composites showed no significant change in the volume fraction of PDMS in the composites, as well as the limited regional stress concentration, resulted from the AgNWs, thereby showing similar stretchability to those of CNT/PEDOT:PSS/PDMS composites.

According to the rule of mixture [35],

$$E_c = f_m E_m + f_f E_f \quad (1)$$

where E_c , E_m , E_f , f_m , and f_f are the modulus of composite, matrix, filler, and the fraction of matrix and filler, respectively. The elastic modulus of the PDMS is expected to increase as the hard fillers such as PEDOT:PSS or CNT are added. Fig. 4b shows the change in the elastic modulus of PDMS composites depending on the added fillers. The elastic modulus, E , was calculated by using a general equation,

$$E = \frac{\sigma}{\varepsilon}, \quad (2)$$

where σ and ε are stress and strain values extracted from the stress-strain curves in Fig. 4a. Pure PDMS showed a modulus value of $0.9 \text{ MPa} \pm 0.10$, which was in the range of data sheet reported in the previously reported study [36]. With the addition of PEDOT:PSS, the modulus increased to $1.5 \text{ MPa} \pm 0.11$. Because the elastic modulus of PEDOT:PSS was reported as ~2.0 GPa [37], the increased modulus values of the composites were confirmed to be due to the addition of PEDOT:PSS. The modulus of the composites was further increased by the addition of CNTs, which showed a $2.0 \text{ MPa} \pm 0.12$ [38]. The elastic modulus of CNTs is reported to be ~900 GPa [39]; thus, even the small addition of CNTs (~2 wt%) resulted in a dramatic increase in the modulus of the composites. The partial embedding of AgNWs only on the surface of the composites showed no significant change in the modulus values; thus, it showed a similar value of $2.0 \text{ MPa} \pm 0.11$ to those of CNT/PEDOT:PSS/PDMS composites. Because of the increased elastic modulus of the composites, the stress values at the same level of a strain of the composites was much higher than those of the pure PDMS. Meanwhile, the rupture stress of the composites was smaller than those of the pure PDMS since the failure of the composites occurred at the much lower strain than those of pure PDMS. However, the rupture strain of the AgNW-coated CNT/PEDOT:PSS/PDMS composites still showed a sufficient value of ~102% for wearable devices, where ~70% strain is considered to be the maximum strain values exerted by human motion [40].

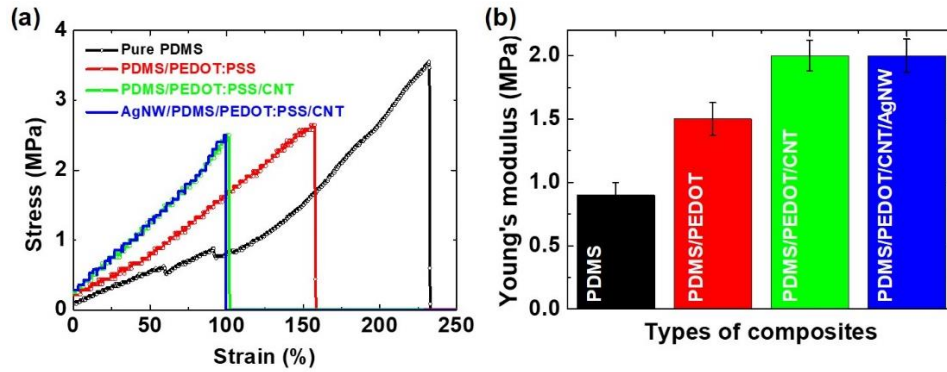


Fig. 4 (a) Stress-strain curves and (b) Young's modulus of PDMS composites using different types of functional fillers.

Fig. 5a shows the electro-mechanical response of the AgNW-coated CNT/PEDOT:PSS/PDMS composites as a function of imposed strain. The resistance value of CNT/PEDOT:PSS/PDMS composites was too high to be used for electrodes of the stretchable supercapacitor, which showed $\sim 1.5 \times 10^6 \Omega/\text{cm}$. The resistance of the composites decreased to $\sim 11.7 \Omega/\text{cm}$ by coating the AgNWs. Therefore, the coating of AgNWs on the composite was necessary to fabricate the stretchable composite electrode using CNT/PEDOT:PSS/PDMS composites. The AgNW-coated CNT/PEDOT:PSS/PDMS composite was highly stretchable under tensile strain. There was no obvious change in the resistance up to the strain of 40%. The resistance started to increase from the strain value over 40%, and from the 50% of strain, a rapid increase in the resistance was observed. Considering that the conductivity of the composites was largely contributed by the AgNWs, the increase in the resistance over 50% of strain was attributed to the loss of the percolation of the AgNW networks by the stretching. Fig. 5b and 5c show the top-view SEM images of AgNW-coated CNT/PEDOT:PSS/PDMS composites under 40% and 60% of tensile strains, respectively. There was no trace of cracks or failure of the composites under 40% of strain as shown in Fig. 5b. At the 60% strain, however, the composites clearly showed failures on the surface (Fig. 5c). Therefore, the AgNW networks on the surface of the composite have been disconnected which resulted in the rapid increase in resistance under the severe tensile strain of over 50%.

The electrochemical performance of AgNW-coated CNT/PEDOT:PSS/PDMS composites was characterized by CV using coin cell configuration with 1 M of Na₂SO₄ aqueous electrolyte (Fig. 6). The CV curve was displayed at a scanning rate of 10 mV/s, 50 mV/s, 100 mV/s, and 200 mV/s under an operation potential window between 0 to 0.8 V. The CV curve was devoid of any redox peaks within a potential range and retained sharp rectangular shapes, demonstrating the typical behavior of an electrical double-layer capacitor. In addition, on increasing scan rate, the shape of the potential window remained similar, and the integrated area of the CV curve increased with the increasing scan rate. This indicates that the supercapacitor has faster charge/discharge capability, verifying the high-rate performance of the supercapacitor. The specific capacitance values were measured to be 248.59 mF/g, 81.77 mF/g, 53.26 mF/g, and 32.55 mF/g at different scan rates of 10 mV/s, 50 mV/s, 100 mV/s, and 200 mV/s, respectively. As the scan rate increases, the specific capacitance value decreased, because of the slower ion diffusion [41]. The AgNW-coated surface was hydrophilic, while the

CNT/PEDOT:PSS/PDMS composite part was more hydrophobic than AgNW coated surface, due to PDMS (Figs. 6b-e). Therefore, the aqueous electrolyte might not sufficiently permeate through the electrode, causing slower ion diffusion.

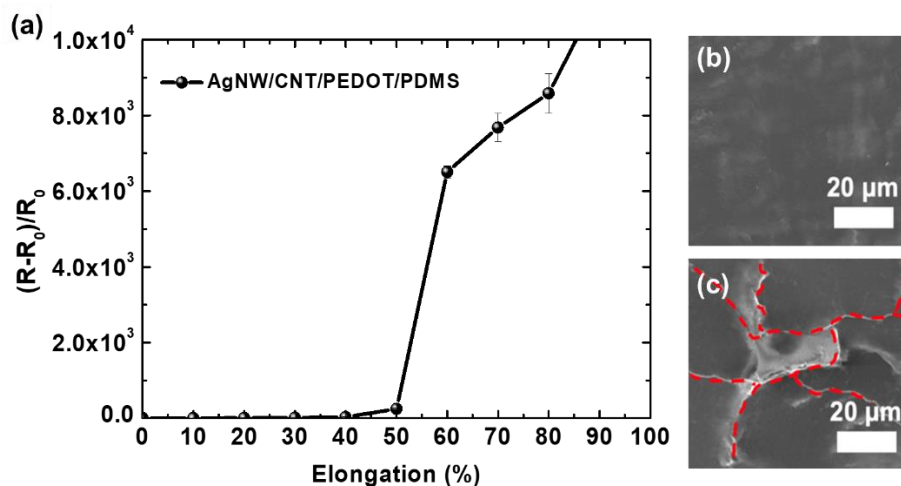


Fig. 5 (a) Normalized resistance change of the AgNW-coated CNT/PEDOT:PSS/PDMS composites as a function of tensile strain values. Top-view SEM images of the AgNW-coated CNT/PEDOT:PSS/PDMS composites under the tensile strain of (b) 40% and (c) 60%.

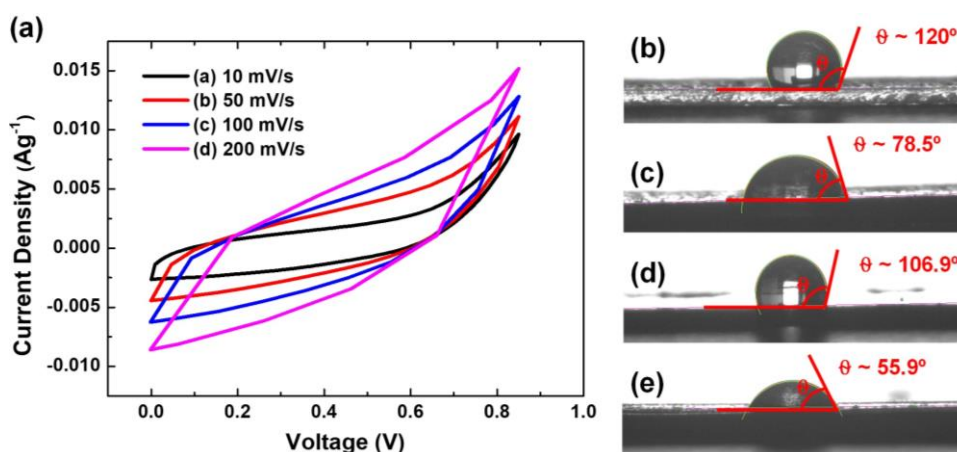


Fig. 6 (a) Cyclic voltammetry (CV) curves for the AgNW coated CNT/PEDOT:PSS/PDMS composite at different scan rates. (b-e) Optical images of water drop shape on (b) pure PDMS, (c) PEDOT:PSS/PDMS, (d) CNT/PEDOT:PSS/PDMS, and (e) AgNW coated CNT/PEDOT:PSS/PDMS.

4. CONCLUSION

In this study, the electro-mechanical response of PDMS composites with hybrid filler were explored. The CNT/PEDOT:PSS/PDMS composite was fabricated via a simple blending method and AgNW was successfully coated on the surface of the composite using the peeling-off method. The fabricated composite not only showed high mechanical reliability under tensile deformation but also maintained electro-mechanical stability, showing a gradual increase in resistance under high elongation values. Moreover, the conductive functional fillers acted effectively as synergetic materials for supercapacitors, demonstrating better electrochemical properties than those using single fillers. The developed AgNW coated CNT/PEDOT:PSS/PDMS composites with high stretchability and mechanical stability, showing better electrochemical performances than those using single fillers demonstrate its possibility of being used for devices that requires electro-mechanical reliability under tensile deformation.

Acknowledgement: This work was supported by a National Research Foundation of Korea (NRF) grant funded by the Korean government (MSIT) (Nos. 2022R1F1A1063696 and 2019K1A3A1A25000230).

REFERENCES

1. Liu, Y., Pharr, M., Salvatore, G.A., 2017, *Lab-on-skin: A review of flexible and stretchable electronics for wearable health monitoring*, ACS Nano, 11(10), pp. 9614-9635.
2. Kim, H., Matteini, P., Hwang, B., 2022, *Mini Review of Reliable Fabrication of Electrode under Stretching for Supercapacitor Application*, Micromachines, 13(9), 1470.
3. Qaiser, N., Al-Modaf, F., Khan, S.M., Shaikh, S.F., El-Atab, N., Hussain, M.M., 2021, *A robust wearable point-of-care cnt-based strain sensor for wirelessly monitoring throat-related illnesses*, Advanced Functional Materials, 31(29), 2103375.
4. Yi, F., Wang, X., Niu, S., Li, S., Yin, Y., Dai, K., Zhang, G., Lin, L., Wen, Z., Guo, H., Wang, J., Yeh, M.-H., Zi, Y., Liao, Q., You, Z., Zhang, Y., Wang, Z.L., 2016, *A highly shape-adaptive, stretchable design based on conductive liquid for energy harvesting and self-powered biomechanical monitoring*, Science Advances, 2(6), e1501624.
5. Wu, H., Huang, Y., Xu, F., Duan, Y., Yin, Z., 2016, *Energy harvesters for wearable and stretchable electronics: From flexibility to stretchability*, Advanced Materials, 28(45), pp. 9881-9919.
6. Wang, Y., Ding, Y., Guo, X., Yu, G., 2019, *Conductive polymers for stretchable supercapacitors*, Nano Research, 12(9), pp. 1978-1987.
7. Yoon, H., Kim, H., Matteini, P., Hwang, B., 2022, *Suspension with Surfactants in Their Application as Electrodes of Batteries: A Mini-Review*, Batteries, 8(12), 254.
8. Christoe, M.J., Han, J., Kalantar-Zadeh, K., 2020, *Telecommunications and data processing in flexible electronic systems*, Advanced Materials Technologies, 5(1), 1900733.
9. Hussain, A.M., Hussain, M.M., 2016, *Cmos-technology-enabled flexible and stretchable electronics for internet of everything applications*, Advanced Materials, 28(22), pp. 4219-4249.
10. Harris, K.D., Elias, A.L., Chung, H.J., 2016, *Flexible electronics under strain: A review of mechanical characterization and durability enhancement strategies*, Journal of Materials Science, 51(6), pp. 2771-2805.
11. Luo, R., Li, H., Du, B., Zhou, S., Zhu, Y., 2020, *A simple strategy for high stretchable, flexible and conductive polymer films based on pedot:Pss-pdms blends*, Organic Electronics, 76, 105451.
12. Seo, Y., Ko, S., Ha, H., Qaiser, N., Leem, M., Yoo, S.J., Jeong, J.H., Lee, K., Hwang, B., 2022, *Stretchable carbonyl iron powder/polydimethylsiloxane composites for noise suppression in gigahertz bandwidth*, Composites Science and Technology, 218, 109150.
13. Matsuhisa, N., Chen, X., Bao, Z., Someya, T., 2019, *Materials and structural designs of stretchable conductors*, Chemical Society Reviews, 48(11), pp. 2946-2966.
14. Qaiser, N., Khan, S.M., Nour, M., Rehman, M.U., Rojas, J.P., Hussain, M.M., 2017, *Mechanical response of spiral interconnect arrays for highly stretchable electronics*, Applied Physics Letters, 111(21), 214102.

15. Qaiser, N., Damdam, A.N., Khan, S.M., Shaikh, S.F., Hussain, M.M., 2019, *Design, mechanics, and operation of spiral-interconnect based networked sensor for stretchable electronics*, Applied Physics Letters, 115(18), 181904.
16. Qaiser, N., Damdam, A.N., Khan, S.M., Bunaiyan, S., Hussain, M.M., 2021, *Design criteria for horseshoe and spiral-based interconnects for highly stretchable electronic devices*, Advanced Functional Materials, 31(7), 2007445.
17. Widlund, T., Yang, S., Hsu, Y.-Y., Lu, N., 2014, *Stretchability and compliance of freestanding serpentine-shaped ribbons*, International Journal of Solids and Structures, 51(23), pp. 4026-4037.
18. Nasreldin, M., Delattre, R., Marchiori, B., Ramuz, M., Maria, S., Tocnaye, J.L.d.B.d.l., Djenizian, T., 2019, *Microstructured electrodes supported on serpentine interconnects for stretchable electronics*, APL Materials, 7(3), 031507.
19. Guo, C.F., Sun, T., Liu, Q., Suo, Z., Ren, Z., 2014, *Highly stretchable and transparent nanomesh electrodes made by grain boundary lithography*, Nature Communications, 5(1), 3121.
20. Yun, G., Tang, S.-Y., Lu, H., Zhang, S., Dickey, M.D., Li, W., 2021, *Hybrid-filler stretchable conductive composites: From fabrication to application*, Small Science, 1(6), 2000080.
21. Przybyłek, P., Opara, T., Kucharczyk, W., Żurowski, W., Pietras, A., 2022, *Simulation of operating loads of ablative composite shields used in flight data recorders*, Reports in Mechanical Engineering, 3(1), pp. 145-157.
22. Hwang, B., Yun, T.G., 2019, *Stretchable and patchable composite electrode with trimethylolpropane formal acrylate-based polymer*, Composites Part B: Engineering, 163, pp. 185-192.
23. Sidhu, A.S., 2021, *Surface texturing of non-toxic, biocompatible titanium alloys via electro-discharge*, Reports in Mechanical Engineering, 2(1), pp. 51-56.
24. Onyibo, E.C., Safaei, B., 2022, *Application of finite element analysis to honeycomb sandwich structures: A review*, Reports in Mechanical Engineering, 3(1), pp. 192-209.
25. Hwang, B., Han, Y., Matteini, P., 2022, *Bending fatigue behavior of ag nanowire/cu thin-film hybrid interconnects for wearable electronics*, Facta Universitatis, Series: Mechanical Engineering, 20(3), pp. 553-560.
26. Lee, M.-S., Lee, K., Kim, S.-Y., Lee, H., Park, J., Choi, K.-H., Kim, H.-K., Kim, D.-G., Lee, D.-Y., Nam, S., Park, J.-U., 2013, *High-performance, transparent, and stretchable electrodes using graphene-metal nanowire hybrid structures*, Nano Letters, 13(6), pp. 2814-2821.
27. Shi, J., Li, X., Cheng, H., Liu, Z., Zhao, L., Yang, T., Dai, Z., Cheng, Z., Shi, E., Yang, L., Zhang, Z., Cao, A., Zhu, H., Fang, Y., 2016, *Graphene reinforced carbon nanotube networks for wearable strain sensors*, Advanced Functional Materials, 26(13), pp. 2078-2084.
28. Yun, G., Tang, S.-Y., Sun, S., Yuan, D., Zhao, Q., Deng, L., Yan, S., Du, H., Dickey, M.D., Li, W., 2019, *Liquid metal-filled magnetorheological elastomer with positive piezoconductivity*, Nature Communications, 10(1), 1300.
29. Seo, Y., Ha, H., Cheong, J.Y., Leem, M., Darabi, S., Matteini, P., Müller, C., Yun, T.G., Hwang, B., 2022, *Highly reliable yarn-type supercapacitor using conductive silk yarns with multilayered active materials*, Journal of Natural Fibers, 19(3), pp. 835-846.
30. Chodankar, N.R., Pham, H.D., Nanjundan, A.K., Fernando, J.F.S., Jayaramulu, K., Golberg, D., Han, Y.-K., Dubal, D.P., 2020, *True meaning of pseudocapacitors and their performance metrics: Asymmetric versus hybrid supercapacitors*, Small, 16(37), 2002806.
31. Yoon, H., Matteini, P., Hwang, B., 2023, *Effect of the Blade-Coating Conditions on the Electrical and Optical Properties of Transparent Ag Nanowire Electrodes*, Micromachines, 14(1), 114.
32. Babita, Sharma, S.K., Gupta, S.M., 2018, *Synergic effect of sdb and ga to prepare stable dispersion of cnt in water for industrial heat transfer applications*, Materials Research Express (Online), 5(5), 12.
33. Lin, Y.-J., Ni, W.-S., Lee, J.-Y., 2015, *Effect of incorporation of ethylene glycol into PEDOT:PSS on electron phonon coupling and conductivity*, Journal of Applied Physics, 117(21), 215501.
34. Yoon, S.-S., Khang, D.-Y., 2016, *Roles of nonionic surfactant additives in PEDOT:PSS thin films*, The Journal of Physical Chemistry C, 120(51), pp. 29525-29532.
35. Yerbolat, G., Amangeldi, S., Ali, M.H., Badanova, N., Ashirbeok, A., Islam, G., 2018, *Composite materials property determination by rule of mixture and monte carlo simulation*, 2018 IEEE International Conference on Advanced Manufacturing (ICAM), 2018, pp. 384-387.
36. Sepúlveda, A.T., Fachin, F., Villoria, R.G.d., Wardle, B.L., Viana, J.C., Pontes, A.J., Rocha, L.A., 2011, *Nanocomposite flexible pressure sensor for biomedical applications*, Procedia Engineering, 25, pp. 140-143.
37. Tahk, D., Lee, H.H., Khang, D.-Y., 2009, *Elastic moduli of organic electronic materials by the buckling method*, Macromolecules, 42(18), pp. 7079-7083.
38. Kumar Singaravel, D., Sharma, S., Kumar, P., 2022, *Recent progress in experimental and molecular dynamics study of carbon nanotube reinforced rubber composites: A review*, Polymer-Plastics Technology and Materials, 61(16), pp. 1792-1825.
39. Loos, M.R., Manas-Zloczower, I., 2012, *Reinforcement efficiency of carbon nanotubes – myth and reality*, Macromolecular Theory and Simulations, 21(2), pp. 130-137.

40. Hu, Y., Zhao, T., Zhu, P., Zhang, Y., Liang, X., Sun, R., Wong, C.-P., 2018, *A low-cost, printable, and stretchable strain sensor based on highly conductive elastic composites with tunable sensitivity for human motion monitoring*, *Nano Research*, 11(4), pp. 1938-1955.
41. Li, Y., Zhao, X., Xu, Q., Zhang, Q., Chen, D., 2011, *Facile preparation and enhanced capacitance of the polyaniline/sodium alginate nanofiber network for supercapacitors*, *Langmuir*, 27(10), pp. 6458-6463.